ISSN 1674-1056
http://cpb.iphy.ac.cn
http://iopscience.iop.org/cpb
中国物理 B
Chinese Physics
中国物理 Chinese Physics B

# InP quantum dots-based electroluminescent devices

Qianqian Wu(吴倩倩), Fan Cao(曹璠), Lingmei Kong(孔令媚), Xuyong Yang(杨绪勇)
**Citation:**Chin. Phys. B . 2019, 28(11): 118103 . **doi:** 10.1088/1674-1056/ab4cdb
Journal homepage: http://cpb.iphy.ac.cn; http://iopscience.iop.org/cpb

**What follows is a list of articles you may be interested in**

---

## Modulation of magnetic and electrical properties of bilayer graphene quantum dots using rotational stacking faults

Hong-Ping Yang(杨宏平), Wen-Juan Yuan(原文娟), Jun Luo(罗俊), Jing Zhu(朱静)
Chin. Phys. B . 2019, 28(7): 078106 . **doi:** 10.1088/1674-1056/28/7/078106

## Molecular beam epitaxial growth of high quality InAs/GaAs quantum dots for 1.3-μ quantum dot lasers

Hui-Ming Hao(郝慧明), Xiang-Bin Su(苏向斌), Jing Zhang(张静), Hai-Qiao Ni(倪海桥), Zhi-Chuan Niu(牛智川)
Chin. Phys. B . 2019, 28(7): 078104 . **doi:** 10.1088/1674-1056/28/7/078104

## 1.3-μm InAs/GaAs quantum dots grown on Si substrates

Fu-Hui Shao(邵福会), Yi Zhang(张一), Xiang-Bin Su(苏向斌), Sheng-Wen Xie(谢圣文), Jin-Ming Shang(尚金铭), Yun-Hao Zhao(赵云昊), Chen-Yuan Cai(蔡晨元), Ren-Chao Che(车仁超), Ying-Qiang Xu(徐应强), Hai-Qiao Ni(倪海桥), Zhi-Chuan Niu(牛智川)
Chin. Phys. B . 2018, 27(12): 128105 . **doi:** 10.1088/1674-1056/27/12/128105

## Facilitative effect of graphene quantum dots in $MoS_2$ growth process by chemical vapor deposition

Lu Zhang(张璐), Yongsheng Wang(王永生), Yanfang Dong(董艳芳), Xuan Zhao(赵宣), Chen Fu(付晨), Dawei He(何大伟)
Chin. Phys. B . 2018, 27(1): 018101 . **doi:** 10.1088/1674-1056/27/1/018101

## Electric-field-dependent charge delocalization from dopant atoms in silicon junctionless nanowire transistor

Hao Wang(王昊), Wei-Hua Han(韩伟华), Xiao-Song Zhao(赵晓松), Wang Zhang(张望), Qi-Feng Lyu(吕奇峰), Liu-Hong Ma(马刘红), Fu-Hua Yang(杨富华)
Chin. Phys. B . 2016, 25(10): 108102 . **doi:** 10.1088/1674-1056/25/10/108102

---

TOPICAL REVIEW — Quantum dot displays

# InP quantum dots-based electroluminescent devices*

Qianqian Wu(吴倩倩)[1,2], Fan Cao(曹璠)[2], Lingmei Kong(孔令媚)[1,2], and Xuyong Yang(杨绪勇)[2,†]

[1] School of Material Science and Engineering, Shanghai University, Shanghai 200072, China
[2] Key Laboratory of Advanced Display and System Applications of Ministry of Education, Shanghai University, Shanghai 200072, China

(Received 20 August 2019; revised manuscript received 10 September 2019; published online 25 October 2019)

Indium phosphide (InP) quantum dots (QDs) have shown great potential to replace the widely applied toxic cadmium-containing and lead perovskite QDs due to their similar emission wavelength range and emission peak width but without intrinsic toxicity. Recently, electrically driven red and green InP-based quantum-dot light-emitting diodes (QLEDs) have achieved great progress in external quantum efficiency (EQE), reaching up to 12.2% and 6.3%, respectively. Despite the relatively poor device performance comparing with cadmium selenide (CdSe)- and perovskite-based QLEDs, these encouraging facts with unique environmental friendliness and solution-processability foreshadow the enormous potential of InP-based QLEDs for energy-efficient, high-color-quality thin-film display and solid-state lighting applications. In this article, recent advances in the research of the InP-based QLEDs have been discussed, with the main focus on device structure selection and interface research, as well as our outlook for on-going strategies of high-efficiency InP-based QLEDs.

**Keywords:** indium phosphide, quantum dots, light-emitting diodes, external quantum efficiency

**PACS:** 81.07.Ta, 85.35.Be, 85.30.de **DOI:** 10.1088/1674-1056/ab4cdb

## 1. Introduction

Since the first advent of semiconductor quantum dots (QDs) about three decades ago, they have attracted a great deal of attention due to their outstanding photoelectric properties such as tunable emission, narrow full-width at half-maximum (FWHM), saturated color, high quantum efficiency and solution-based processing methods.[1–6] Of all types of QDs, only cadmium selenide (CdSe) and lead perovskite QDs satisfy the requirements of optical display technologies.[7–11] However, the inherent toxicity of CdSe/perovskite QDs and the instability of perovskite QDs have severely limited the application and development of the QDs. The growing demand for non-toxic and eco-friendly QDs has greatly stimulated the enthusiasm of researchers.[12–16] InP is of great importance as a potential substitute for toxic Cd-based and lead perovskite QDs due to its lower toxicity and similar optical properties.[17–21] Recently, remarkable improvements have been made with the synthesis of core-shell-type InP QDs, where the highest photoluminescence quantum yield (PLQY) of 90% for green with FWHM of 35 nm and 95% for red with FWHM of 42 nm was achieved by the core-shell-type InP QDs.[22] These breakthroughs provide the possibility for fabricating high-efficiency InP-based quantum-dot light-emitting diodes (QLEDs), with the peak external quantum efficiency (EQE) of 12.2% for red and 6.3% for green, respectively. This fact proves that the great prospects of InP QD application in electroluminescence (EL), combined with uniquely size-tunable color and solution-processable foreshadow the potential of InP-based QLEDs for energy-efficient, high-color-quality thin-film display and solid-state lighting applications.

This article aims to provide an illustrative account on recent progress of InP-based QLEDs. The basic theories and fundamental properties of InP colloidal QDs are similar to those of Cd-containing QDs and have been well described in many comprehensive reviews. Here, we focus on high-efficiency InP-based QLEDs, including device structure design, charge transport layer material selection, optimization, and mechanism research.

## 2. Design principles for efficient InP-based QLEDs

Through in-depth research on the chemical and device mechanisms of Cd-containing QD, the performance of the device has been dramatically enhanced. However, compared to highly developed Cd-based technologies, research on Cd-free QLEDs in the past five years is still far behind, especially with InP-based QDs, and there are remained critical challenges.

In general, the EQE of a QLED is defined as the ratio of the number of photons emitted by the QLED to free space to the number of injected charge carriers (i.e., EQE $= N_{\text{emitting photons}}/N_{\text{injected electrons}}$). In order to better understand the device mechanism, several parameters can be used

*Project supported by the National Natural Science Foundation of China (Grant Nos. 51675322, 61605109, and 61735004), the National Key Research and Development Program of China (Grant No. 2016YFB0401702), Shanghai Science and Technology Committee, China (Grant No. 19010500600), Shanghai Rising-Star Program, China (Grant No. 17QA1401600), and the Program for Professor of Special Appointment (Eastern Scholar) at Shanghai Institutions of Higher Learning, China.

†Corresponding author. E-mail: yangxy@shu.edu.cn

© 2019 Chinese Physical Society and IOP Publishing Ltd 

to describe the EQE

$$\eta_{\mathrm{eqe}} = \eta_{\mathrm{i}}\eta_{\mathrm{oc}} = \gamma\varphi_{\mathrm{QY}}\chi\eta_{\mathrm{oc}},$$

where $\eta_{\mathrm{eqe}}$ is the EQE, $\eta_{\mathrm{i}}$ is the internal quantum efficiency (IQE), $\eta_{\mathrm{oc}}$ is the light out-coupling efficiency, $\gamma$ is the charge carrier balance factor which includes the carrier injection and transport efficiency, $\varphi_{\mathrm{QY}}$ is the internal luminescent quantum yield (QY), and $\chi$ is the spin-allowed optical transition rate. $\chi$ is assumed to be 100% for QDs due to the heavy atom mediated spin–orbit coupling in the heavy metal center, or the efficient crossing of excitons from the 'dark' states to higher energy 'bright' states. $\eta_{\mathrm{oc}}$ is typically found to be c.a. 20% for planar devices. Therefore, the important parameters to enhance the device efficiency are the charge carrier balance factor ($\chi$) and the internal luminescent QY ($\varphi_{\mathrm{QY}}$). To obtain high EQE, the design principles of the InP-based QLEDs are as follows.

**Principle 1** From the luminescent materials perspective, the PLQY of the InP QD should be as high as possible.

**Principle 2** From the device structure perspective, the electron and hole injections into the QDs layer should be as balanced as possible.

Specifically, in order to obtain high PLQY ($\varphi_{\mathrm{QY}}$) of InP QD, a lattice-matched multilayer shell structure was utilized, which not only effectively limits the electron and hole wave functions to the core, but also passivates the QDs' surface defects. The carrier balance factor ($\gamma$), corresponding with carrier mobility and material stability, also plays a crucial role for high-quality InP QDs. Furthermore, an appropriate charge transport layer (CTL) with a low injection barrier for the QD should be carefully selected.

## 3. Compositions of electrically driven InP-based QLEDs

In QLEDs, the QDs layer is typically sandwiched between the hole transport layer (HTL) and the electron transport layer (ETL). The CTL not only is responsible for promoting the charge injection into the QDs layer, but also affects other basic processes of the QLED operation. The charge injection efficiency depends on the conductivity of the CTL and the alignment of the electrode/CTL with the energy level of the QD/CTL interface. Effective exciton formation requires charge-selective CTLs with good blocking properties to achieve efficient charge limitation within the QDs layer and sensible modulation of the electron/hole injection to achieve charge balance. In general, ETLs can employ the i) organic layer: 2, 2′, 2″-(1, 3, 5-benzinetrily) tris(1-phenyl-1-H-benzimidazole) (TPBi), or ii) inorganic layers: ZnO or $ZrO_2$.[23–25] HTLs usually employ the organic layers including poly(9-vinlycarbazole) (PVK), poly(N, N′-bis(4-butylphenyl)-N, N′-bis(phenyl)-benzidine) (poly-TPD), or poly [(9, 9-dioctylfluorenyl-2, 7-diyl)-co-(4, 4′-(N-(p-butylphenyl))diphenylamine)] (TFB).

Over the past several years, many researchers have focused on the improvement of electroluminescent devices utilizing InP-based QDs. Electrically driven InP-based QLEDs have increased in EQE from less than 0.01% to around 12%. These breakthroughs inspire researchers to keep exploring environmentally friendly InP QLED.

### 3.1. Developing highly efficient conventional InP-based QLEDs

A typical high efficient, conventional InP-based QLED structure includes: ITO/hole injection layer (HIL)/HTL/InP QDs/ETL/cathode. For solution processed InP-based QLEDs, the selection of appropriate solvents is very critical for achieving the spin-coated functional layers without any damage. Preventing solvent corrosion and mixing of multilayer devices is a fundamental requirement for obtaining high performance QLEDs. Therefore, it must be ensured that adjacent functional layers use orthogonal solvents to avoid erosion. Poly(ethylenedioxythiophene): polystyrene sulphonate (PEDOT: PSS) is one of the most commonly used HIL which performs as the anode buffer layer to enhance the work function and reduce the surface roughness of the ITO substrate.[26] As for HTL, the materials include PVK, poly-TPD, and TFB. ETLs can be TPBi, ZnO, or ZnMgO. The material of the cathode is usually Ag or Al.

In 2012, an interesting report by Sun and co-workers demonstrated a white QLED with a high color rendering index of 91 based on InP QDs.[27,28] Detailed structure of the device is shown in Fig. 1. The thin film of poly-TPD is chemically and physically stable to nonpolar alkane solvents so that the QDs can simply be spin-coated on top of the poly-TPD layer. TPBi is used as the ETL because it has a suitable lowest unoccupied molecular orbital (LUMO) energy and a good hole blocking layer. The loosely packed QD layer design results in direct contact between poly-TPD and TPBi, a ternary complementary white QLED consisting of blue component (poly-TPD), green component (InP QD), and red component (exciplex formed at the interface between poly-TPD and TPBi) has been shown with a high color rendering index of 91, which successfully attracted researchers to study high-performance, low-toxic InP QD in lighting displays.

Recently, ZnO or metal doped ZnO nanoparticles (NPs) are the most widely used electron transport material due to their efficient electron injection and transport properties. Here we focus on ZnO NPs, which are widely used as ETL in the state-of-the-art high-performance InP-based QLEDs. To cite an example, figures 2(a) and 2(b) show a device structure consisting of Al, ZnO NPs, TFB, PEDOT: PSS, and ITO as the cathode, ETL, HTL, HIL, and anode, respectively.[29] The work reported that the QLEDs based on thick-shell InP

QDs showed a peak EQE of 6.3% and a current efficiency (CE) of over 13.7 cd/A, which is the highest record for green-emitting InP-based QLEDs. The choice of the hole transport material will also greatly affect the performance of the device. Yang and co-workers compared the performance of PVK- and TFB-based all solution-processed InP-based QLEDs. Although compared with TFB, PVK may help the HTL–QDs layer hole injection from the perspective of energy arrangement. However, since the hole mobility of TFB ($\sim 10^{-2}$ $cm^2 \cdot V^{-1} \cdot s^{-1}$) is relatively higher than that of PVK ($10^{-6}$–$10^{-5}$ $cm^2 \cdot V^{-1} \cdot s^{-1}$),[30,31] the TFB-based device has a much higher current density than the PVK-based one within the same voltage, therefore, not only can the turn-on voltage be effectively reduced, but also the maximum luminance of the device can be improved.[32] Experimental data is shown in Figs. 2(c) and 2(d), in the case of the PVK-based QLED, the CE, EQE, and power efficiency (PE) collected at the low luminance level of 20 cd/m$^2$ (4.5 V) were 2.5 cd/A, 1.4%, and 1.8 lm/W, respectively. At the same time, the TFB-based QLED showed a greatly enhanced maximum current of 4.2 cd/A in CE, 2.5% in EQE, and 4.4 lm/W in PE at an even higher luminance of 1008 cd/m$^2$ (3 V).

Besides ZnO-based all solution-processed QLEDs, the fabrication of Mg-doped ZnO-based devices has also attracted much attention. Recently, Peng and his co-works reported a red-emitting all solution-process conventional QLED having record-breaking device performance with maximum luminance of over 10000 cd/m$^2$, high EQE of 12.2%, and excellent reproducibility. Detailed structure of the device is shown in Fig. 3. It is close to the red-emitting QLED based on CdSe QDs.[22] It has been documented that the visible emission of ZnO originates from the presence of defect centers, in particular due to the radiation recombination of shallow trap electrons and the vacancies of oxygen vacancies trapped in the interstitial state.[5,33] Mg-doped ZnO forms ZnMgO, which not only makes the size of the NPs smaller, but also reduces the defect state of ZnO in the visible light band.[34] Mg-doped ZnO helps to reduce the trapping of electrons and holes by the defect states, thereby improving the efficiency of the device.

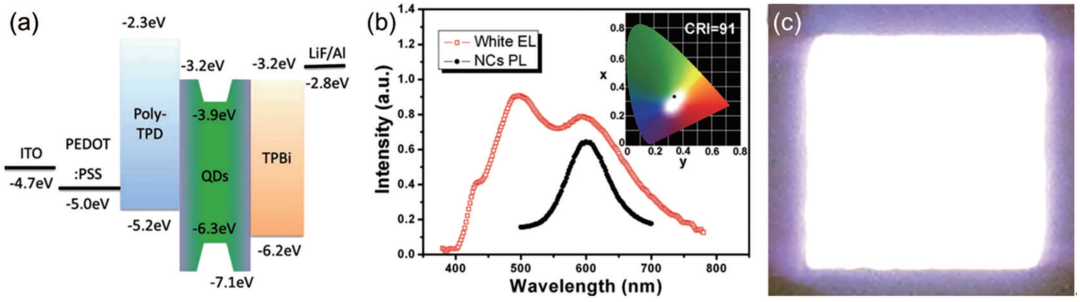



**Fig. 1.** (a) Energy band diagram of the QLEDs using InP/ZnS QDs. (b) PL spectrum of red-emitting InP/ZnS NCs and EL spectrum of white QLEDs. (c) CIE chromaticity coordinate diagram of the white QLEDs and a photograph of a QLED with a pixel size of 3 mm × 3 mm (inset). Reproduced with permission.[24] Copyright 2012, Wiley.

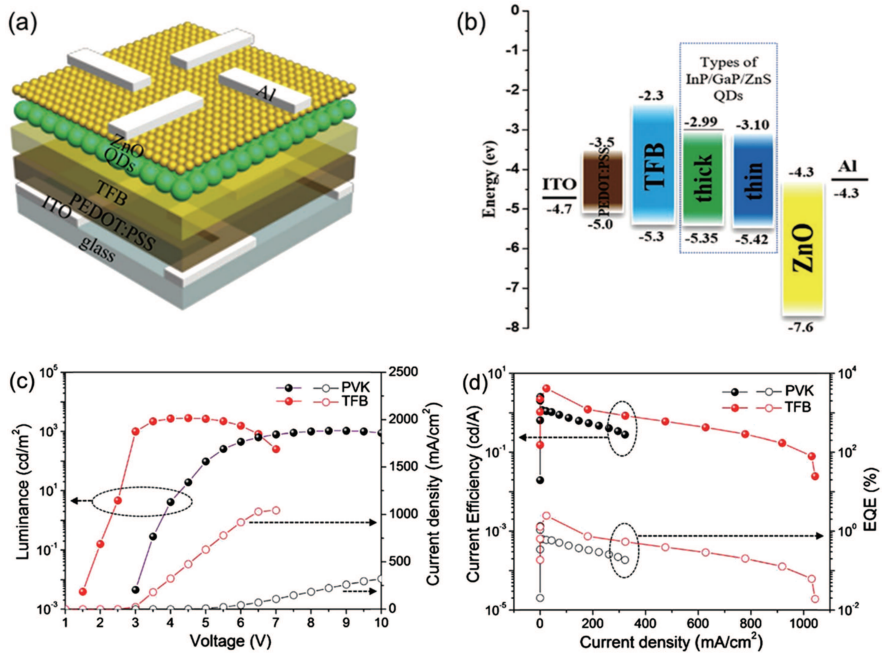



**Fig. 2.** (a) Schematic diagram of the QLEDs structure. (b) Energy level illustration for materials used in the QLEDs. Reproduced with permission.[29] Copyright 2019, Wiley. Variations of (c) current density–voltage–luminance (*J*–*V*–*L*) and (d) CE–*J*–EQE of PVK- and TFB-based QLEDs. Reproduced with permission.[32] Copyright 2016, The Optical Society.

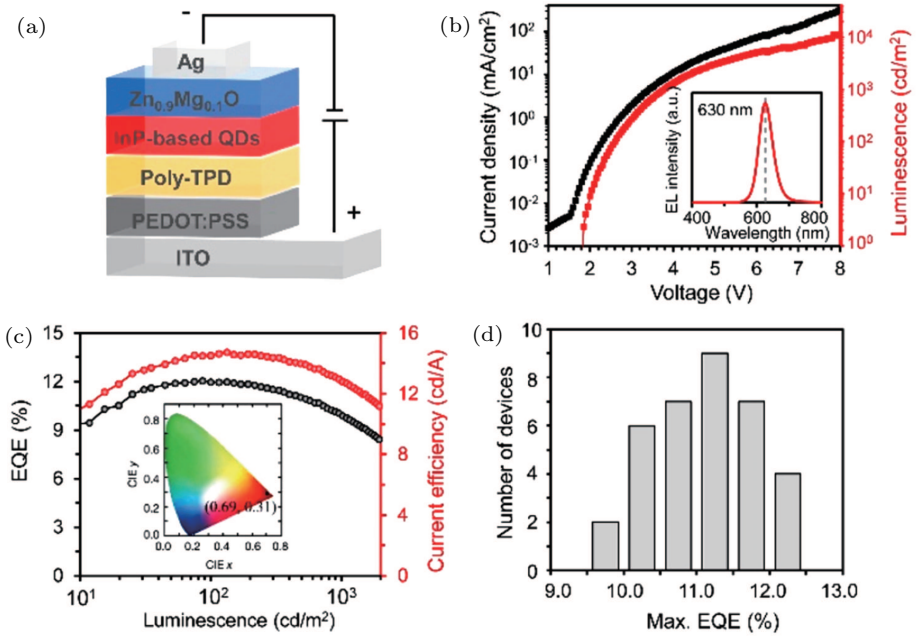



**Fig. 3.** (a) Scheme of the QLEDs. (b) *J*–*V*–*L* for the optimal device. Inset: EL spectrum. (c) EQE–*L*–CE of the optimal device. Inset: corresponding CIE coordinates. (d) Histogram of peak EQEs for 35 devices. Reproduced with permission.[22] Copyright 2019, American Chemical Society.

### 3.2. Developing high efficient inverted InP-based QLEDs

A typical high efficient, inverted InP-based QLED structure includes: ITO/ZnO or doped-ZnO/InP QDs/HTLs/anode. Since HTLs usually use organic materials and require temperature annealing of 100 °C or more. However, the current InP QD still cannot withstand high temperature conditions. Therefore, in a highly efficient inverted InP-based device, HTL is generally achieved by evaporation. In our previous work, a highly efficient red-emitting InP-based QLED with a structure of ITO/ZnO/QDs/4, 4′-bis(carbazol-9-yl)biphenyl (CBP)/dipyrazino [2, 3-f: 2′, 3′-h]-quinoxaline-2, 3, 6, 7, 10, 11-hexacarbonitrile (HAT-CN)/Al was reported as shown in Fig. 4.[35] HAT-CN is selected as the HIL of the inverted QLED because the injection efficiency of the inverted device with the HAT-CN top contact HIL is near unity.[36] CBP ($\sim 2\times10^{-3}$ cm$^2$·V$^{-1}$·s$^{-1}$) is chosen as the HTL because it has a sufficiently high hole mobility comparable to the electron mobility of ZnO ($\sim 1.8\times10^{-3}$ cm$^2$·V$^{-1}$·s$^{-1}$).[6,37] The matched concentrations of electrons and holes in the luminescent layer will greatly reduce the blinking phenomenon caused by charging of the QDs, which is beneficial to the improvement of the device performance.[38] Figures 4(d) and 4(e) show the device's *J*–*V*–*L* and CE–*L*–EQE characteristics. Among them, the maximum luminance exceeding 1600 cd/m$^2$ is achieved at an applied voltage of 8.5 V. The peak CE of 13.6 cd/A corresponds to an EQE of 6.6%. The histogram of the peak EQE shows an average peak EQE of 5.27%, showing excellent repeatability (Fig. 4(f)).

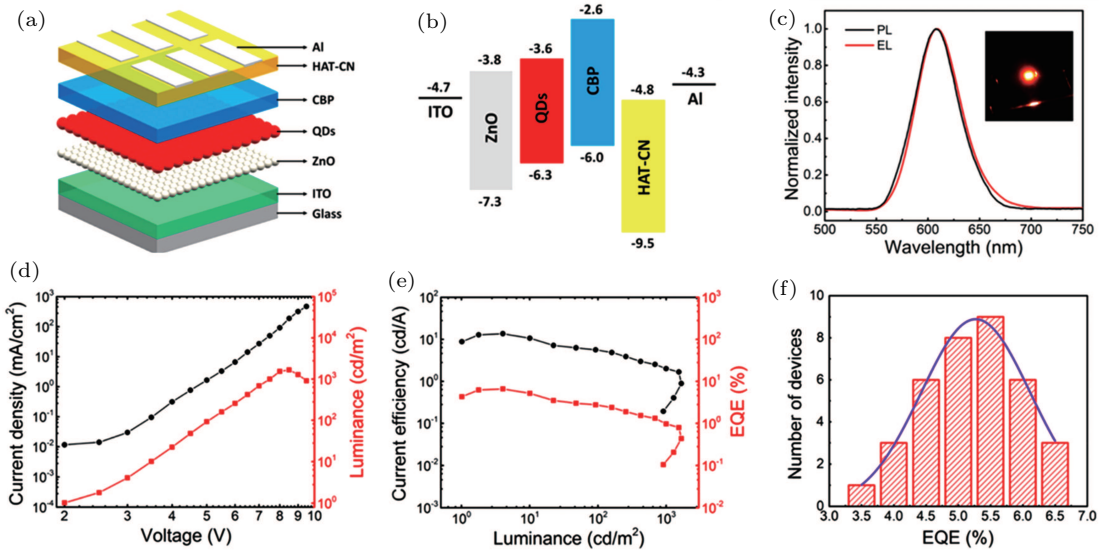



**Fig. 4.** (a) Schematic device structure of multilayered InP QLED and (b) energy levels of individual layers of the device. (c) Normalized EL and PL spectra, *J*–*V*–*L* and CE–*L*–EQE characteristics of the device. (f) Histogram of peak EQEs measured from 36 devices. Reproduced with permission.[35] Copyright 2018, American Chemical Society.

In 2015, Wedel and co-workers reported the use of polyethyleneimine (PEI) surface modifiers to increase the efficiency of InP-based QLEDs.[39] The cross-section schematic and energy band diagram of the inverted QLEDs are shown in Fig. 5. The leakage current of the inverted device was substantially suppressed by adjusting the solution-processed PEI layer on top of the Al-doped zinc oxide (Al: ZnO) NPs film. In addition, the electron injection into the conduction band edge (CBE) of the InP/ZnSe/ZnS QDs was also facilitated by the low work function (WF) of the Al: ZnO film which was realized by the strong interfacial dipoles of the thin film of PEI. As a result, the charge balance in the inverted devices was controlled by the change of surface roughness, the WF of the ETL, and the combination of different thicknesses of PEI interfacial layer with the oxide layer, so that the CE was dramatically increased from 0.07 cd/A to 3.17 cd/A. It shows the great potential of using an interfacial dipole layer to develop highly efficient InP-based inverted QLEDs. Poly-[(9, 9-bis(30-(N, N-dimethylamino)propyl)-2, 7-fluorene)-alt-2, 7-(9, 9-ioctylfluorene)] (PFN) has similar functions to PEI, both of them contain an amino group that can have a strong interaction with the surface of the semiconductor, providing a large positive interface dipole moment. As a result, significant vacuum levels shift to lower energy at the interface.[40,41] For example, Char and co-workers reported the introduction of a thin layer of PFN at the interface between ZnO and InP QDs to reduce the electron injection barrier. The PFN conjugated polyelectrolytes are used as interface dipole layers and are known to achieve vacuum level shifts over 0.5 eV.[23]

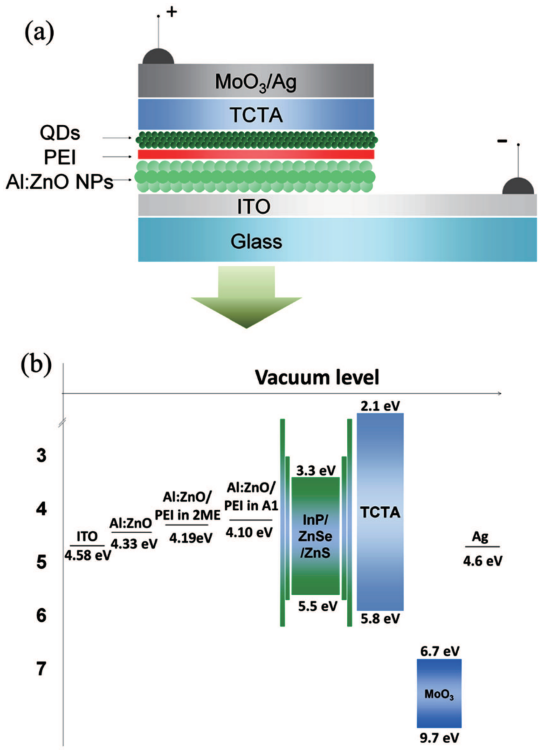



**Fig. 5.** (a) A cross-section schematic and (b) an energy band diagram of the inverted QLEDs. Reproduced with permission.[39] Copyright 2015, Society for Information Display.

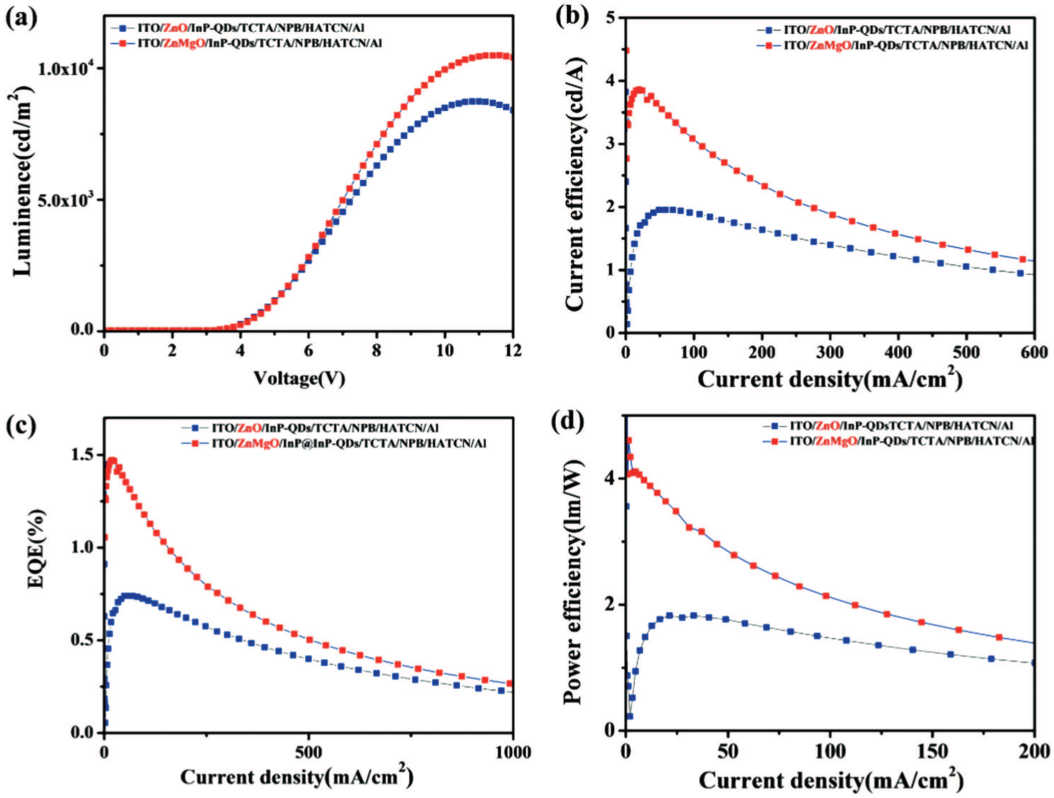



**Fig. 6.** Device characteristics of the inverted InP/ZnSeS/ZnS QLEDs with different ETLs: (a) luminance as a function of applied bias, (b) CE–*J*, (c) EQE–*J*, and (d) PE–*J* spectra of this device.[42] Reproduced with permission. Copyright 2017, Wiley.

Mg-doped ZnO has better electron transport properties than undoped ZnO, which has been confirmed in the above-mentioned conventional devices. The introduction of ZnMgO into inverted devices can still promote better device performance. For example, Liu and co-workers reported an inverted QLED based on high PLQY and stable thick-shelled green InP/ZnSeS/ZnS QDs.[42] By comparing the InP-based QLEDs with ZnO or ZnMgO as the electron transport layers, it is proved that ZnMgO as the electron transport layer can inject electrons into the QDs layer more effectively. When the applied bias voltage was over 10 V, the InP-based QLED containing ZnO ETL began to decay. By contrast, the InP-based QLED with the ZnMgO layer maintained a luminance of over 10 V, indicating that the ZnMgO layer also improved the charge balance and device stability at high voltage. The CE, EQE, and PE of this device are shown in Fig. 6. For the device with the ZnMgO ETL, these values were nearly twofold higher than those of the device with the ZnO ETL. The optimized inverted InP/ZnSeS/ZnS QLEDs exhibited a low turn-on voltage (2.2 V) and a maximum luminescence of 10490 cd/m$^2$. The PE and CE were 3.63 lm/W and 3.86 cd/A, respectively, at 1000 cd/m$^2$. These results indicated that the proposed InP-based QLEDs also performed well under high luminance.

### 3.3. Efficient transparent flexible InP-based QLED

Flexible information displays hold great promise for future optoelectronic applications. For efficient transparent flexible InP-based QLEDs, Bae and co-workers adopted an inverted QLED architecture, in which the InP QDs layer is sandwiched between tris(4-carbazoyl-9-ylphenyl)amine (TCTA)/$MoO_x$/Al and PFN/ZnO/ITO (Fig. 7(a)).[43] In this work, TCTA was employed as HTL to reduce the hole injection barrier. Besides, TCTA could serve as effective electron blocking layer because of the low electron mobility and high LUMO level. Figures 7(b)–7(e) show the optoelectronic characteristics of green- and red-emitting QLEDs. Both QLEDs exhibit turn-on voltages close to the optical bandgap of the QDs, indicating that the charge carriers are easily drifted into the QD emitting-layer and recombine to emit photons. Both QLEDs show EL with the narrow FWHM in the green and red regions (CIE$(x,\ y) = (0.24, 0.72)$ and $(0.70,\ 0.30)$), and the peak EQE is 3.78% and 3.92% and the peak luminance is 2504 cd/m$^2$ and 6881 cd/m$^2$, respectively. We note that the color purity and luminance of the current version of the device satisfactorily meet the requirements of the display. Oh and co-workers proposed the InP QLEDs with bottom emission structure and inorganic $ZrO_2$ nanoparticles as the electron transport layer in 2016.[25] To realize the transparent QLED display, the two-step sputtering process of indium zinc oxide (IZO) top electrode was applied to the devices and this study could achieve the fabrication of transparent QLED device with the transmittance of higher than 74% for the whole device array, this interesting work makes InP-based transparent QLED become a promising device for the next generation of transparent display.

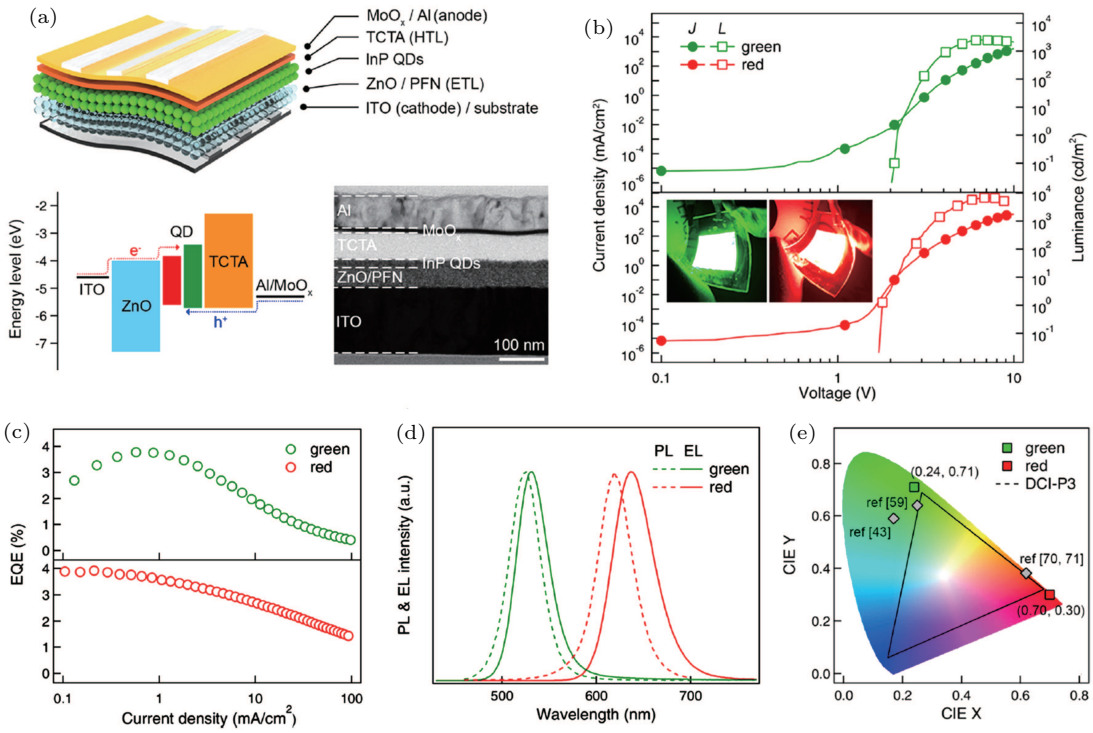



**Fig. 7.** (a) Schematic illustration (top), the energy band diagram (bottom, left), and a cross-sectional TEM image (bottom, right) of QLED. (b) $J$–$V$–$L$ characteristics (inset: photographs of green- and red-emitting QLEDs), (c) EQE–$J$, and (d) EL spectra of green- and red-emitting QLEDs. PL spectra of green- and red-emitting QDs are overlaid for comparison. (e) The color coordinates of EL spectra of green- and red-emitting QLEDs in the CIE 1931 color space chromaticity diagram.[43] Copyright 2019, American Chemical Society.

## 4. Conclusions and perspective

InP-based QLED technology has unprecedented potential for environmentally friendly, energy-saving, wide color-gamut, and flexible displays. Attractive progress has been made in material chemistry of QDs and CTLs and device engineering of QLEDs. Even though many researches on InP-based QLEDs in recent years, the advances on device architecture and related mechanisms are not comparable with those of highly developed techniques based on Cd-based QLEDs. From the point of view of device structure engineering, and the understanding of fundamental device mechanism, this paper provides experimental guidance and theoretical insights for the designing of InP-based QLEDs. The following perspectives are critical to accelerate the commercialization of this exciting technology: (i) the performance for red and green InP-based QLEDs needs to be further improved to catch up with Cd-based QLEDs, (ii) the developments of efficient blue InP QDs and their QLEDs are inferior to those of the state-of-the-art green and red QLEDs. It is difficult to efficiently inject carriers into blue QDs due to their wide bandgap, corresponding with energy transfer in the QD films, interface charge transfer between blue QDs and CTLs, and electric field induced quenching in blue QLEDs.

## References


[1] Cho K S, Lee E K, Joo W J, Jang E, Kim T H, Lee S J, Kwon S J, Han J Y, Kim B K, Choi B L and Kim J M 2009 *Nat. Photon.* **3** 341
[2] Wang C, Shim M and Guyot-Sionnest P 2001 *Science* **291** 2390
[3] Qian L, Zheng Y, Xue J and Holloway P H 2011 *Nat. Photon.* **5** 543
[4] Shirasaki Y, Supran G J, Bawendi M G and Bulović V 2013 *Nat. Photon.* **7** 13
[5] Mashford B S, Stevenson M, Popovic Z, Hamilton C, Zhou Z, Breen C, Steckel J, Bulovic V, Bawendi M, Coe-Sullivan S and Kazlas P T 2013 *Nat. Photon.* **7** 407
[6] Dai X, Zhang Z, Jin Y, Niu Y, Cao H, Liang X, Chen L, Wang J and Peng X 2014 *Nature* **515** 96
[7] Shen H, Gao Q, Zhang Y, Lin Y, Lin Q, Li Z, Chen L, Zeng Z, Li X, Jia Y, Wang S, Du Z, Li L S and Zhang Z 2019 *Nat. Photon.* **13** 192
[8] Lin K, Xing J, Quan L N, de Arquer F P G, Gong X, Lu J, Xie L, Zhao W, Zhang D, Yan C, Li W, Liu X, Lu Y, Kirman J, Sargent E H, Xiong Q and Wei Z 2018 *Nature* **562** 245
[9] Walters G, Wei M, Voznyy O, Quintero-Bermudez R, Kiani A, Smilgies D M, Munir R, Amassian A, Hoogl S and Sargent E 2018 *Nat. Commun.* **9** 4214
[10] Supran G J, Shirasaki Y, Song, K W, Caruge J M, Kazlas P T, Coe-Sullivan S, Andrew T L, Bawendi M G and Bulović V 2013 *MRS Bull.* **38** 703
[11] Zheng J J, Wang Y R, Yu K H, Xu X X, Sheng X X, Hu E T and Wei W 2018 *Acta Phys. Sin.* **67** 118502 (in Chinese)
[12] Anc M J, Pickett N L, Gresty N C, Harris J A and Mishra K C 2013 *ECS J. Solid State Sci. Technol.* **2** R3071
[13] Derfus A M, Chan W C and Bhatia S N 2004 *Nano Lett.* **4** 11
[14] Hardman R 2006 *Environ. Health Perspect.* **114** 165
[15] Luo S, Ji H M, Gao F, Yang X G, Liang P, Zhao L J and Yang T 2013 *Chin. Phys. Lett.* **30** 068101
[16] Yang G Q, Zhang S Z, Xu B, Chen Y H and Wang Z G 2017 *Chin. Phys. B* **26** 068103
[17] Tamang S, Lincheneau C, Hermans Y, Jeong S and Reiss P 2016 *Chem. Mater.* **28** 2491
[18] Battaglia D and Peng X 2002 *Nano Lett.* **2** 1027
[19] Byun H J, Song W S and Yang H 2011 *Nanotechnology* **22** 235605
[20] Ramasamy P, Kim N, Kang Y S, Ramirez O and Lee J S 2017 *Chem. Mater.* **29** 6893
[21] Buffard A, Dreyfuss S, Nadal B, Heuclin H, Xu X, Patriarche G, Mézailles N and Dubertret B 2016 *Chem. Mater.* **28** 5925
[22] Li Y, Hou X, Dai X, Yao Z, Lv L, Jin Y and Peng X 2019 *J. Am. Chem. Soc.* **141** 6448
[23] Lim J, Park M, Bae W K, Lee D, Lee S, Lee C and Char K 2013 *ACS Nano* **7** 9019
[24] Ramasamy P, Ko K J, Kang J W and Lee J S 2018 *Chem. Mater.* **30** 3643
[25] Kim H Y, Park Y J, Kim J, Han C J, Lee J, Kim Y, Greco T, Ippen C, Wedel A, Ju B K and Oh M S 2016 *Adv. Funct. Mater.* **26** 3454
[26] Cheng T, Wang Z, Jin S, Wang F, Bai Y, Feng H, You B, Li Y, Hayat T and Tan Z A 2017 *Adv. Opt. Mater.* **5** 1700035
[27] Yang X, Zhao D, Leck K S, Tan S T, Tang Y X, Zhao J, Demir H V and Sun X W 2012 *Adv. Mater.* **24** 4180
[28] Yang X, Divayana Y, Zhao D, Leck K S, Lu F, Tan S T, Abiyasa A P, Zhao Y, Demir H V and Sun X W 2012 *Appl. Phys. Lett.* **101** 233110
[29] Zhang H, Hu N, Zeng Z, Lin Q, Zhang F, Tang A, Jia Y, Li L S, Shen H, Teng F and Du Z 2019 *Adv. Opt. Mater.* **7** 1801602
[30] Yang Y, Zheng Y, Cao W, Titov A, Hyvonen J, Manders J R, Xue J, Holloway P H and Qian L 2015 *Nat. Photon.* **9** 259
[31] Ho M D, Kim D, Kim N, Cho S M and Chae H 2013 *ACS Appl. Mater. Interfaces* **5** 12369
[32] Jo J H, Kim J H, Lee K H, Han C Y, Jang E P, Do Y R and Yang H 2016 *Opt. Lett.* **41** 3984
[33] Van Dijken A, Meulenkamp E A, Vanmaekelbergh D and Meijerink A 2000 *J. Phys. Chem. B* **104** 1715
[34] Kim J H, Han C Y, Lee K H, An K S, Song W, Kim J, Oh M S, Do Y R and Yang H 2014 *Chem. Mater.* **27** 197
[35] Cao F, Wang S, Wang F, Wu Q, Zhao D and Yang X 2018 *Chem. Mater.* **30** 8002
[36] Small C E, Tsang S W, Kido J, So S K and So F 2012 *Adv. Funct. Mater.* **22** 3261
[37] Kirkwood N, Singh B and Mulvaney P 2016 *Adv. Mater. Interfaces* **3** 1600868
[38] Yuan G, Gomez D E, Kirkwood N, Boldt K and Mulvaney P 2018 *ACS Nano* **12** 3397
[39] Kim Y, Ippen C, Fischer B, Lange A and Wedel A 2015 *J. Soc. Inf. Disp.* **23** 377
[40] Kim D, Fu Y, Kim S, Lee W, Lee K H, Chung H K, Lee H J, Yang H and Chae H 2017 *ACS Nano* **11** 1982
[41] Wu H, Huang F, Peng J and Cao Y 2005 *Org. Electron.* **6** 118
[42] Wang H C, Zhang H, Chen H Y, Yeh H C, Tseng M R, Chung R J, Chen S and Liu R S 2017 *Small* **13** 1603962
[43] Hahm D, Chang J H, Jeong B G, Park P, Kim J, Lee S, Choi J, Kim W D, Rhee S, Lim J, Lee D C, Lee C, Char K and Bae W K 2019 *Chem. Mater.* **31** 3476